

Robust Monitoring of Time Series with Application to Fraud Detection

Peter Rousseeuw, Domenico Perrotta, Marco Riani and Mia Hubert

May 22, 2018

Abstract

Time series often contain outliers and level shifts or structural changes. These unexpected events are of the utmost importance in fraud detection, as they may pinpoint suspicious transactions. The presence of such unusual events can easily mislead conventional time series analysis and yield erroneous conclusions. A unified framework is provided for detecting outliers and level shifts in short time series that may have a seasonal pattern. The approach combines ideas from the FastLTS algorithm for robust regression with alternating least squares. The double wedge plot is proposed, a graphical display which indicates outliers and potential level shifts. The methodology was developed to detect potential fraud cases in time series of imports into the European Union, and is illustrated on two such series.

Keywords: alternating least squares, double wedge plot, level shift, outliers.

Peter Rousseeuw, Department of Mathematics, University of Leuven, Belgium. Domenico Perrotta, Joint Research Centre, Ispra, Italy. Marco Riani, Department of Economics, University of Parma, Italy. Mia Hubert, Department of Mathematics, University of Leuven, Belgium. Peter Rousseeuw and Mia Hubert gratefully acknowledge the support by project C16/15/068 of Internal Funds KU Leuven. The work of Domenico Perrotta was supported by the Project “Automated Monitoring Tool on External Trade Step 5” of the Joint Research Centre and the European Anti-Fraud Office of the European Commission, under the Hercule-III EU programme. In this paper, references to specific countries and products are made only for purposes of illustration and do not necessarily refer to cases investigated or under investigation by anti-fraud authorities.

1 Introduction

When analyzing time series one often encounters unusual events such as outliers and structural changes, like those in Figure 1. Both series track trade volumes, and were extracted from the official trade statistics in the COMEXT database of Eurostat. This database contains monthly trade volumes (aggregated over several transactions, possibly involving different traders) of products imported in the European Union (EU) in a four-year period. The plot titles in Figure 1 specify the code of the traded product in the EU Combined Nomenclature classification (CN code), the country of origin, and the destination (a member state of the EU). The CN code determines whether the volumes are expressed in tons of net mass and/or other units (liters, number of items, etc.), the rate of customs duty applied, and how the goods are treated for statistical purposes. The data quality is quite heterogeneous across countries and products, but some macroscopic outliers (manifest errors) have already been removed or corrected by statistical authorities and customs services.

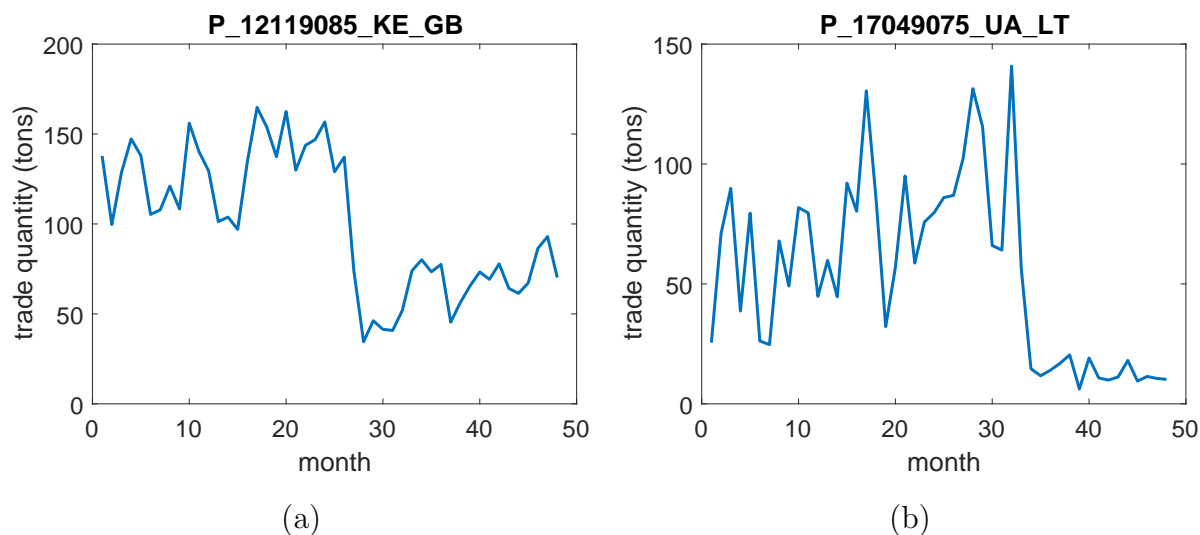


Figure 1: Monthly trade volumes of two products imported in the European Union in a four-year period: (a) imports of plants used primarily in perfumery, pharmacy or for insecticidal, fungicidal or similar purposes, from Kenya into the UK (P12119085-KE-GB); (b) import of sugars including chemically pure lactose, maltose, glucose and fructose, sugar syrups, artificial honey and caramel, from the Ukraine into Lithuania (P17049075-UA-LT).

Both of these time series exhibit a downward level shift. Knowing when such structural

breaks occur is important for fraud detection. For instance, a sudden reduction in trade volume may coincide with an increase for a related product or another country of origin, which could indicate a misdeclaration with the intent of deflecting customs duties.

There are many products and countries of origin in the CN classification, but not all of these combinations occur and the number of products at risk of fraud is relatively small. Still, the number of relevant combinations of a product at fraud risk, a country of origin and a country of destination is around 16,000. As a result, every month around 16,000 time series need to be analyzed for anti-fraud purposes. This requires an automatic approach that is able to report accurate information on outliers and the positions and amplitudes of level shifts, and that runs fast enough for that time frame. The method proposed in this paper meets those objectives, and provides a graphical display that can be looked at whenever the automatic monitoring system detects a significant level shift. Our method follows the approach which first computes a robust fit to the majority of the data and then detects outliers by their large residuals, as described in the review paper (Rousseeuw and Hubert, 2018).

A different statistical approach to monitor international trade data for fraud was proposed by Barabesi et al. (2016) who tested whether the distribution of trade volumes follows the Newcomb-Benford law. In the current paper we also take the time sequence of the trades into account. We will focus on a parametric approach to estimate level shifts, which differs from the nonparametric smoothing methods in Fried and Gather (2007) or robust methods for REGARIMA models (Bianco et al., 2001). A popular technique is the X13 ARIMA-SEATS Seasonal Adjustment methodology (Findley et al., 1998; U.S. Census Bureau, 2017). X-13 is based on automatic fitting of ARIMA models and includes detection of additive outliers and level shifts. We will compare our results with those of X-13 in Section 5. See also Galeano and Peña (2013) for a review of robust modeling of linear and nonlinear time series.

Although this paper was motivated by the need to analyze many short time series of trade data, we will describe the methodology more generally so it can be applied to other types of time series that may be longer and can be modeled with more parameters.

The structure of the paper is as follows. In Section 2 we introduce our model and

methodology for robustly analyzing a time series which contains a trend, a seasonal component and possibly a level shift in an unknown position, as well as isolated or consecutive outliers. In Section 3 we illustrate the proposed approach using the well-known airline data (Box and Jenkins, 1976), as well as contaminated versions of it in order to test the ability of the method to detect anomalies. In this section we also introduce the double wedge plot, which visualizes the presence of a level shift and outliers. In Section 4 we apply our methodology to the time series in Figure 1. Section 5 compares our results to those obtained by a nonparametric method and to X-13. The case where more than one level shift occurs is discussed in Section 6. Section 7 concludes, and the Appendix proves a result about our algorithm.

2 Methodology

2.1 The model

The time series $y(t) = y_t$ (for $t = 1, \dots, T$) we will consider may contain the following terms:

1. a polynomial trend, i.e. $\sum_{a=0}^A \alpha_a t^a$;
2. a seasonal component, i.e.

$$S_t = \sum_{b=1}^B \left(\beta_{b,1} \cos \left(\frac{2\pi b}{12} t \right) + \beta_{b,2} \sin \left(\frac{2\pi b}{12} t \right) \right) . \quad (1)$$

When $B = 1$ this is periodic with a one-year period, $B = 2$ corresponds with a six-month period etc. We assume the amplitude of the seasonal component varies over time in a polynomial way, i.e. $y_t \sim \left(1 + \sum_{g=1}^G \gamma_g t^g \right) S_t$;

3. a level shift in an unknown time point $2 \leq \delta_2 \leq T$, i.e. $\delta_1 I(t \geq \delta_2)$ with $I(\cdot)$ the indicator function.

The general model is thus of the form

$$y_t = \sum_{a=0}^A \alpha_a t^a + \left[\sum_{b=1}^B \left(\beta_{b,1} \cos \left(\frac{2\pi b}{12} t \right) + \beta_{b,2} \sin \left(\frac{2\pi b}{12} t \right) \right) \right] \left(1 + \sum_{g=1}^G \gamma_g t^g \right) + \delta_1 I(t \geq \delta_2) + \varepsilon_t . \quad (2)$$

One may assume that the irregular component ε_t of the non-outliers is a stationary random process with $E[\varepsilon_t] = 0$ and $\sigma^2 = \text{Var}[\varepsilon_t] < \infty$. Let us collect all unknown parameters in a vector $\theta = (\alpha_0, \alpha_1, \dots, \beta_{1,1}, \beta_{1,2}, \dots, \gamma_1, \gamma_2, \dots, \delta_1, \delta_2)$ of length p . Then model (2) can be written as

$$y_t = f(\theta, t) + \varepsilon_t$$

with $f(\theta, t) = \sum_{a=0}^A \alpha_a t^a + S_t(1 + \sum_{g=1}^G \gamma_g t^g) + \delta_1 I(t \geq \delta_2)$. The model does not need to contain all of these components, as some coefficients can be zero.

2.2 The nonlinear LTS estimator

Model (2) is nonlinear in the parameters $\beta_{b,1}$, $\beta_{b,2}$, γ_g and δ_2 . As there may be outliers in the time series, we propose to estimate θ by means of the *nonlinear least trimmed squares* (NLTS) estimator (Rousseeuw, 1984; Stromberg and Ruppert, 1992; Stromberg, 1993):

$$\hat{\theta}_{\text{NLTS}} = \underset{\theta}{\operatorname{argmin}} \sum_{j=1}^h r_{(j)}^2(\theta) \quad (3)$$

where $T/2 \leq h < T$ and $r_{(j)}^2(\theta)$ is the j -th smallest squared residual $(y_t - f(\theta, t))^2$. Our default choice for h is $[0.75 T]$.

The \sqrt{n} -consistency and asymptotic normality of NLTS were studied by Čížek (2005, 2008). To compute the estimator, we propose to combine ideas from the FastLTS algorithm for robust linear regression (Rousseeuw and Van Driessen, 2006) with the alternating least squares (ALS) method.

We first describe how we use the alternating least squares procedure. We temporarily assume that the estimated shift time $\hat{\delta}_2$ is fixed, and that we want to solve (3) for a subset of the y_t with at least $p - 1$ observations, at least one of which is to the left of $\hat{\delta}_2$ and at least one of which is equal or to the right of $\hat{\delta}_2$. We denote the indices of the subset as $E \subset \{1, 2, \dots, T\}$ with $\#E \geq p - 1$, where E must overlap with $\{1, \dots, \hat{\delta}_2 - 1\}$ as well as $\{\hat{\delta}_2, \dots, T\}$. These conditions are required to make the parameters in (2) identifiable from the subset $y_E = \{y_t; t \in E\}$. We then go through the following steps:

1. **[Initialization]** Set $\gamma_g = 0$ for $g = 1, \dots, G$. Then a part of (2) drops out, leaving

$$y_t = \sum_{a=0}^A \alpha_a t^a + \sum_{b=1}^B \left(\beta_{b,1} \cos\left(\frac{2\pi b}{12} t\right) + \beta_{b,2} \sin\left(\frac{2\pi b}{12} t\right) \right) + \delta_1 I(t \geq \hat{\delta}_2) + \varepsilon_t \quad (4)$$

which is linear in the parameters α_a , $\beta_{b,1}$, $\beta_{b,2}$ and δ_1 . By applying linear LS to the subset y_E , we obtain the initial estimates $\hat{\alpha}_a^{(0)}$, $\hat{\beta}_{b,1}^{(0)}$, $\hat{\beta}_{b,2}^{(0)}$ and $\hat{\delta}_1^{(0)}$.

2. **[Iteration]** For $k = 1, 2, \dots$ repeat the following steps:

- **[ALS step A]** Let $S_t^{(k-1)} = \sum_{b=1}^B \left(\hat{\beta}_{b,1}^{(k-1)} \cos\left(\frac{2\pi b}{12}t\right) + \hat{\beta}_{b,2}^{(k-1)} \sin\left(\frac{2\pi b}{12}t\right) \right)$ in which the coefficients $\hat{\beta}_{b,1}^{(k-1)}$ and $\hat{\beta}_{b,2}^{(k-1)}$ come from the previous step. Keeping $S_t^{(k-1)}$ fixed yields the model

$$y_t - S_t^{(k-1)} = \sum_{a=0}^A \alpha_a t^a + S_t^{(k-1)} \left(\sum_{g=1}^G \gamma_g t^g \right) + \delta_1 I(t \geq \hat{\delta}_2) + \varepsilon_t \quad (5)$$

which is linear in the parameters α_a , γ_g , and δ_1 . We then apply LS using only the observations in the subset y_E , yielding the estimates $\hat{\alpha}_a^{(k)}$, $\hat{\gamma}_g^{(k)}$ and $\hat{\delta}_1^{(k)}$.

- **[ALS step B]** Keeping the estimated coefficients $\hat{\alpha}_a^{(k)}$, $\hat{\gamma}_g^{(k)}$ and $\hat{\delta}_1^{(k)}$ from the previous step fixed yields the model

$$\begin{aligned} y_t - \sum_{a=0}^A \hat{\alpha}_a^{(k)} t^a - \hat{\delta}_1^{(k)} I(t \geq \hat{\delta}_2) \\ = \left[\sum_{b=1}^B \left(\beta_{b,1} \cos\left(\frac{2\pi b}{12}t\right) + \beta_{b,2} \sin\left(\frac{2\pi b}{12}t\right) \right) \right] \left(1 + \sum_{g=1}^G \hat{\gamma}_g^{(k)} t^g \right) + \varepsilon_t \end{aligned} \quad (6)$$

which is linear in the parameters $\beta_{b,1}$ and $\beta_{b,2}$. We then apply LS using only the observations in the subset y_E , yielding the estimates $\hat{\beta}_{b,1}^{(k)}$ and $\hat{\beta}_{b,2}^{(k)}$. Then we go back to ALS step A.

Let $\hat{\theta}_k$ be the vector of coefficients after iteration step k . We repeat the above steps until $\|\hat{\theta}_k - \hat{\theta}_{k-1}\|/\|\hat{\theta}_{k-1}\|$ is below a threshold, or a maximal number of iterations (say 50) is attained. Here $\|\cdot\|$ is the Euclidean norm.

In words, ALS solves the nonlinear LS problem of fitting (2) to the data set y_E by alternating between the solution of two linear LS fits, (5) and (6).

Our goal is to solve the nonlinear LTS problem (3). A basic tool for linear LTS is the **C-step** (Rousseeuw and Van Driessen, 2006) which we now generalize to the nonlinear setting.

[C-step] Start from a subset $H^{(k)} \subset \{1, 2, \dots, T\}$ to which we fit $\hat{\theta}^{(k)}$ obtained by applying ALS. Then compute the residuals $r_t = y_t - f(\hat{\theta}^{(k)}, t)$ for the whole time series,

that is, for $t = 1, \dots, T$ and not just for $t \in H^{(k)}$. Next retain the h observations with smallest squared residuals, yielding the new subset $H^{(k+1)}$. Then apply ALS to $H^{(k+1)}$, yielding a new fit $\hat{\theta}^{(k+1)}$. It is shown in the Appendix that the new fit $\hat{\theta}^{(k+1)}$ is guaranteed to have a lower objective function than the old fit $\hat{\theta}^{(k)}$. It is possible to iterate the C-step until convergence, which will occur in a finite number of steps.

Using these building blocks, we now describe the entire algorithm to compute the NLTS fit to the model (2). Let $t_{(1)}, \dots, t_{(S)}$ be the ordered indices of the possible positions δ_2 of the level shift, for example the set $\{u + 1, \dots, T - u\}$ for some $u > 0$. The algorithm then consists of the following steps.

1. Loop over all $t_{(s)}$ where $s = 1, \dots, S$ and do:

- (a) Temporarily set $\hat{\delta}_2 = t_{(s)}$.
- (b) Now loop over m ranging from 1 to the number of trial subsets M , and do:
 - i. Construct an elemental subset E containing $p - 1$ different observations. This subset should contain the index $t_{(s)}$, one observation y_t with $t < t_{(s)}$ and $p - 3$ observations drawn at random from the whole time series. Note that we impose that $t_{(s)}$ belongs to E because the purpose of step 1 is to select the most suitable $\hat{\delta}_2 = t_{(s)}$.
 - ii. Run the initialization and ALS steps described above on E , keeping $\hat{\delta}_2 = t_{(s)}$ fixed. Then take two C-steps. [Two C-steps is enough at this stage, in line with the results of Rousseeuw and Van Driessen (2006).] If a singular solution is obtained during the computations, restart without increasing m .

The choice of M is a compromise since the expected number of outlier-free subsets E is proportional to M but the computation speed is inversely proportional to M . In our experiments we found that $M = 250$ was sufficient to obtain stable results.

- (c) Consider only the *nbest* elemental subsets (among the M that were tried) that yielded the lowest objective function so far. Apply C-steps to them until convergence and store these *nbest* solutions. In our examples we found that setting *nbest* to 10 worked well.

- (d) If $s > 1$ also start from the $nbest$ elemental sets found when investigating $t_{(s-1)}$, but this time setting $\hat{\delta}_2 = t_{(s)}$. Apply C-steps to them until convergence.
- (e) Take the fit with the lowest objective among these $2 \times nbest$ candidates, and denote it by $\hat{\theta}^{(s)}$.
- (f) Store the corresponding scaled residuals

$$\tilde{r}_t(\hat{\theta}^{(s)}) = \frac{r_t(\hat{\theta}^{(s)})}{\sqrt{\sum_{t=1}^h r_{(t)}^2(\hat{\theta}^{(s)})/h}} \quad \text{for } t = 1, \dots, T . \quad (7)$$

2. **Retain overall best solution.** Among the fits $\hat{\theta}^{(s)}$ for $s = 1, \dots, S$ take the one with lowest objective function $\sum_{t=1}^h r_{(t)}^2(\hat{\theta}^{(s)})$ and denote it by $\hat{\theta}^{opt}$.

For estimating the scale of the error term we can use $\sum_{t=1}^h r_{(t)}^2(\hat{\theta}^{opt})$. But since this sum of squares only uses the h most central residuals, the estimate needs to be rescaled. The variance $\sigma^2(h)$ of a truncated normal distribution containing the central h/T portion of the standard normal is

$$\sigma^2(h) = 1 - \frac{2T}{h} \Phi^{-1} \left(\frac{T+h}{2T} \right) \phi \left\{ \Phi^{-1} \left(\frac{T+h}{2T} \right) \right\}$$

by equation (6.5) in (Croux and Rousseeuw, 1992). Therefore we compute

$$\tilde{\sigma}^2 = \sum_{t=1}^h r_{(t)}^2(\hat{\theta}^{opt}) / (h\sigma^2(h)) . \quad (8)$$

Note that this makes $\tilde{\sigma}^2$ consistent, but not yet unbiased for small samples. Therefore we include the finite-sample correction factor from Pison et al. (2002) in our final scale estimate $\hat{\sigma}$.

3. **Locally improving the shift position estimate.** The previous steps have yielded an estimate $\hat{\delta}_2$ of the position of the level shift, but it may be imprecise. For instance, it may happen that the h -subset underlying $\hat{\theta}^{opt}$ does not itself contain the time points $\hat{\delta}_2$ or $\hat{\delta}_2 + 1$. In order to improve the estimate we check in its vicinity as follows:

- Take a window W around $\hat{\delta}_2$. For each t^* in W , we replace $\hat{\delta}_2$ by t^* while keeping the other coefficients from $\hat{\theta}^{opt}$ and the scale estimate $\hat{\sigma}$. Compute the residuals

r_t from these coefficients and let $f(t^*) = \sum_{t \in W} \rho(r_t/\hat{\sigma})$ with ρ the Huber function

$$\rho(x) = \begin{cases} x^2/2 & \text{if } |x| \leq b \\ b|x| - b^2/2 & \text{if } |x| > b \end{cases}$$

In our simulations and the analysis of international trade time series (of the kind given in Figure 1) the best results were obtained with b equal to 1.5 or 2. In our implementation the defaults are $b = 2$ and a window W of width 15.

- Our final $\hat{\delta}_2$ is the t^* in W with lowest $f(t^*)$. If it is different from the estimate we had before, we recompute the scaled residuals.
4. **Weighted step.** We apply the univariate outlier detection procedure described in (Gervini and Yohai, 2002) and (Agostinelli et al., 2015) to the T scaled residuals $(y_t - f(\hat{\theta}^{opt}, t))/\hat{\sigma}$. By default we use the 99% confidence level. Alternatively, one could use the thresholds obtained in Salini et al. (2015).
 5. **Final fit.** We apply nonlinear LS to all the points that have not been flagged as outliers in the previous step, starting from the initial estimate $\hat{\theta}^{opt}$ and keeping $\hat{\delta}_2$ fixed. For this we can iterate ALS steps until convergence. The standard errors obtained in the last two ALS steps can be used for inference.

Note that h must be at least the number of parameters p in the model for identifiability. When h is as low as $T/2$ this means $T/p > 2$. However, for stability it is often recommended that $T/p > 5$, see e.g. Rousseeuw and Leroy (1987). The Matlab code of the algorithm can be downloaded from [/www.riani.it/rprh/](http://www.riani.it/rprh/). In the following sections we will apply it to several data sets.

3 Airline data and the double wedge plot

The airline passenger data, given as Series G in Box and Jenkins (1976), has often been used in the time series analysis literature as an example of a nonstationary seasonal time series. It consists of $T = 144$ monthly total numbers of airline passengers from January 1949 to December 1960. Box and Jenkins developed a two-coefficient time series model

of factored form that is now known as the airline model. In this section we will analyze these data using our method, and then contaminate the data in various ways to see how the method reacts.

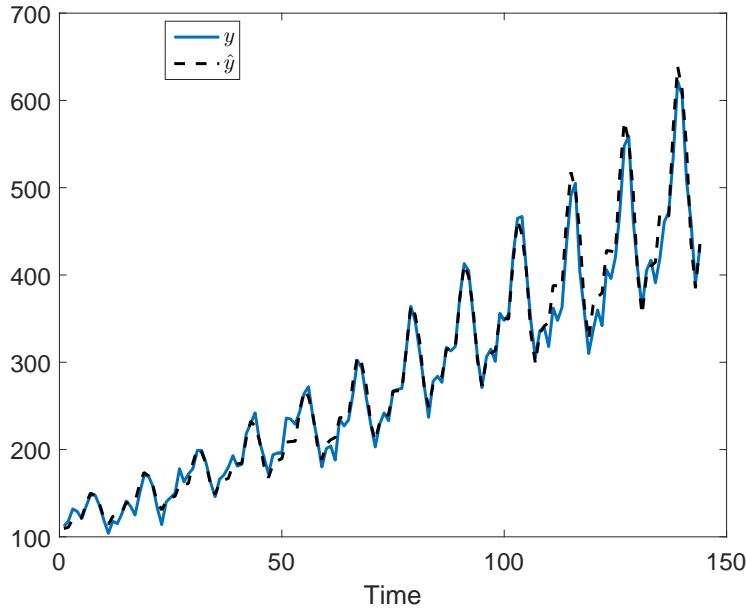


Figure 2: Airline data: observed and fitted values based on model (2) with a quadratic trend, a quarterly seasonal component, and a quadratically varying amplitude.

Uncontaminated data. We fit the data by model (2) with $A = 2$, $B = 4$ and $G = 2$. This means that we assume a quadratic trend, a quarterly seasonal component, and a quadratically varying amplitude. The resulting NLTS fit (3) closely follows the data, as can be seen in Figure 2. In this example no data point has been flagged as outlying. From the standard errors (not shown) we conclude that all coefficients are significant except for the height of the level shift.

Contamination 1. We now contaminate the series by adding three groups of outliers, yielding the blue curve in the bottom panel of Figure 3. More precisely, the value 300 is subtracted from all responses in the interval $[50, 55]$ while 300 is added on $[122, 127]$ and 400 is subtracted on $[130, 134]$. The fitted values (dotted curve) from NLTS closely follow the observed values for the regular observations. The flagged outliers are indicated by red crosses, whose size is proportional to the absolute magnitude of their residual. We see that all the outliers we added are clearly recognized as such, and they were not used to estimate

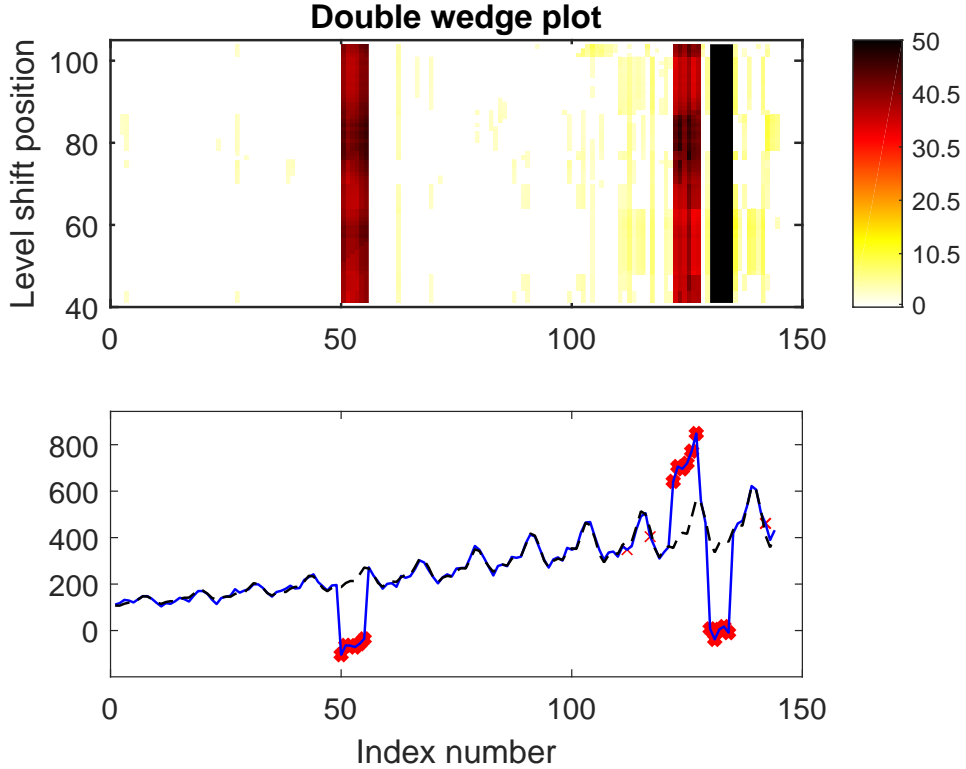


Figure 3: Airline data with contamination 1: double wedge plot (top) and observed and fitted values (bottom).

the coefficients in the weighted step. Only a few regular observations received an absolute residual slightly above the cutoff value.

The top panel of Figure 3 is a byproduct of the algorithm, and is useful for visualizing the presence of (groups of) outliers and a level shift. The first step of the algorithm ranges over all potential positions $t_{(1)}, \dots, t_{(S)}$ of a level shift. These tentative positions $t_{(s)}$ are on the vertical axis. For any $t_{(s)}$ we plot the absolute scaled residuals $|\tilde{r}_t(\hat{\theta}^{(s)})|$ given in (7), in all of the times $t = 1, 2, \dots, T$ on the horizontal axis. The color in the plot depends on the size of that absolute residual and ranges from black (large residuals) over red and yellow to white (small residuals). The color scale is at the right of the plot. Scaled residuals larger than 50 are shown as if they were 50, so that even a very far outlier cannot affect the color coding. In the same spirit, uninformative scaled residuals smaller than 2.5 are shown as if they were 0, so in white. Of course the user can easily modify these default choices.

Outliers have a large absolute scaled residual from the robust fit, so in this plot isolated

outliers will appear as dark vertical lines, and groups of consecutive outliers as dark vertical bands. In this example we clearly see the contamination. The regular observations with scaled residual slightly above 2.5 do not stand out as they are in light yellow.

Contamination 2. In the second contamination setting we introduce a persistent level shift and three isolated outliers, two of which lie in the proximity of the level shift which makes the problem harder. For this we added the value 1300 to all responses from $t = 68$ onward, at $t = 45$ the response is lowered by 800, at $t = 67$ by 600, while at $t = 68$ and $t = 69$ we added an additional 800.

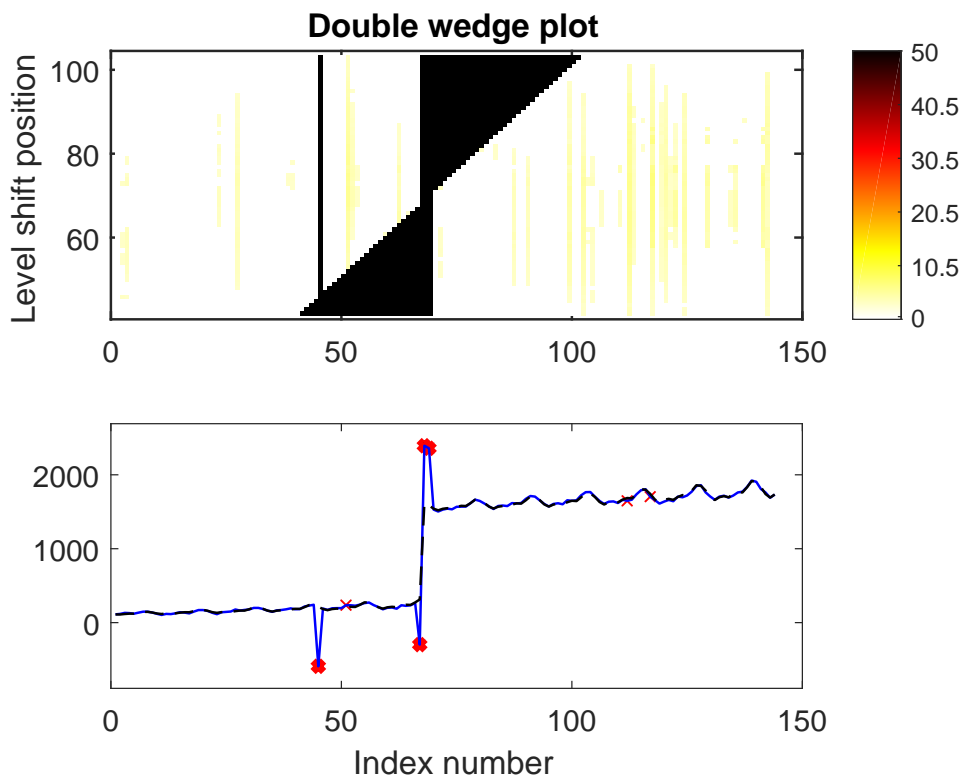


Figure 4: Airline data with contamination 2.

The bottom panel of Figure 4 shows the observed and fitted values. Again all inserted outliers are clearly detected, and a few regular observations have small crosses indicating that their scaled absolute residual was slightly above 2.5.

The plot of the absolute scaled residuals $|\tilde{r}_t(\hat{\theta}^{(s)})|$ in the top panel of Figure 4 now looks more eventful with two dark triangles. Together these ‘wedges’ signal a level shift. To understand this effect, let us assume that the true level shift is at position t^* and the

algorithm is in the process of checking the candidate $t_{(s)} = t^* - r$. Then the algorithm will treat the y_t at $t^* - r + 1, \dots, t^* - 1$ as outliers and the resulting robust fit (still for that $t_{(s)}$) will show $r - 1$ consecutive outliers. Similarly, when the algorithm tries $t_{(s)} = t^* + r$ to the right of t^* , the best solutions will show r outliers. As a result, when approaching the true level shift position t^* from the left the scaled residuals we are monitoring will form a dark upward-pointing wedge, and to the right of the true t^* we obtain an analogous wedge pointing downward. In the top panel of Figure 4. we observe two opposite wedges tapering off in the proximity of the true level shift position, around $t = 68$. In this region we observe a small rectangle (centered at position 68) bridging the two wedges. The rectangle is due to the two outliers in the proximity of the level shift. The isolated outlier at position 45 yields a single dark vertical line like those in Figure 3.

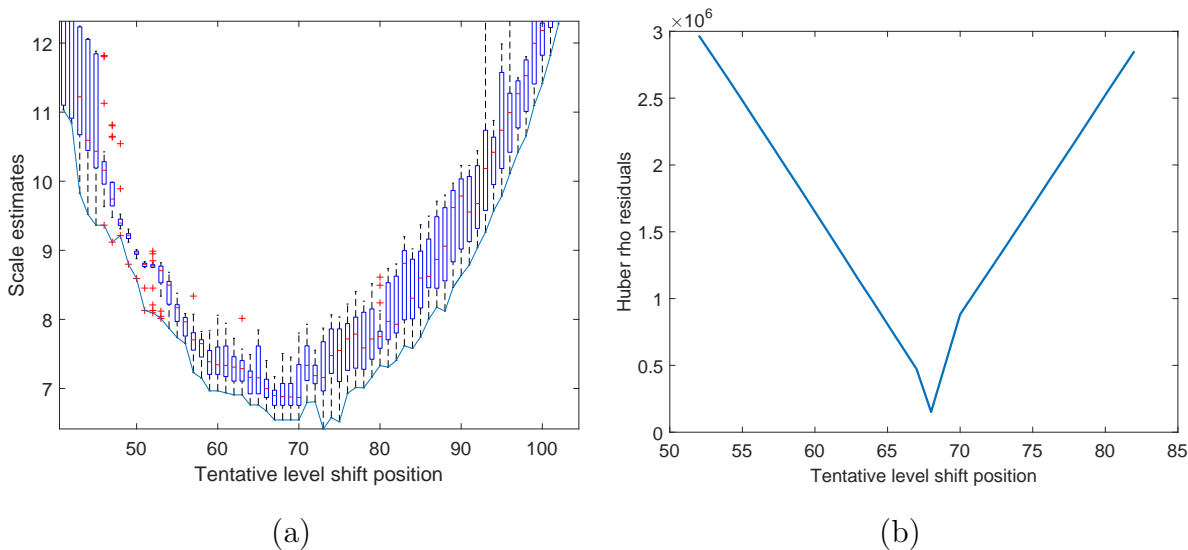


Figure 5: Airline data with contamination 2: (a) boxplots of the 20 lowest objective function values attained at each $t_{(s)}$; (b) local improvement of the shift position estimate.

Panel (a) of Figure 5 shows the boxplots of the objective function $\sum_{t=1}^h r_{(t)}^2(\hat{\theta}_j^{(s)})$ attained by the $2 \times nbest = 20$ best solutions $\hat{\theta}_j$ in step 1(e) of the algorithm. It is thus also a free byproduct of the estimation. If a level shift is present in the central part of the time series, this plot will typically have a U shape. In this example the lowest values of the trimmed sum of squared residuals occur in the time range 60-80. The continuous curve which connects the lowest objective value for each s reaches its global minimum at $t_{(s)} = 73$. However, the curve is quite bumpy in that region, with several local minima and a near-

constant stretch on 67-70, so the position of the minimum is not precise. This kind of situation motivated the local improvement in step 3 of the algorithm. Panel (b) of Figure 5 shows $f(t_{(s)}) = \sum_{t \in W} \rho(r_t / \hat{\sigma})$ as a function of the tentative position $t_{(s)}$ (with ρ the Huber function with $b = 2$) on the interval 53-82. This curve has a much better determined minimum, in fact at $t = 68$, confirming the benefit of the local improvement step.

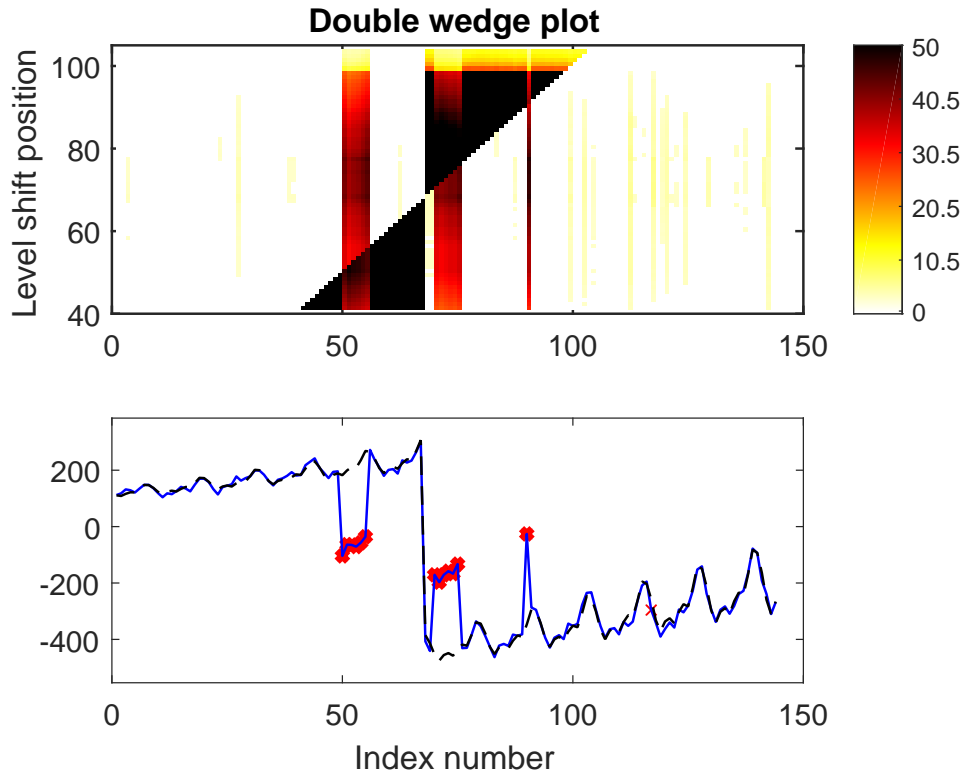


Figure 6: Airline data with contamination 3.

Contamination 3. In the final contaminated dataset we inserted a level shift and a group of consecutive outliers following it. To complicate things even more, we also put in a stretch of contamination to the left of the level shift, as well as an isolated outlier. The bottom panel of Figure 6 shows the robust fit, which succeeded in recovering the structure and flagging the outliers. In the top panel of Figure 6 we see the typical double wedge pattern indicating a level shift. The two reddish bands flag the groups of consecutive outliers, whereas the single line corresponds to the isolated outlier at $t = 90$. In this example the thick end of the upper wedge is yellow, so the absolute scaled residuals are not as large there. This part corresponds to a tentative level shift of around 100, which is

very far from the true one, and in such cases the fit may indeed be quite different.

4 Analysis of trade data

Our main goal is to analyze the many short time series of trade described in Section 1. After trying several model specifications in the class (2) we found that the best results were obtained by using a linear trend, two harmonics, and one parameter to model the varying amplitude of the seasonal component, that is, $A = 1$, $B = 2$ and $G = 1$. Note that this yields $p = 9$ parameters including the position and height of a potential level shift, which is not too many compared to the length of the time series ($T = 48$). As an example we now apply our method to the time series in Figure 1.

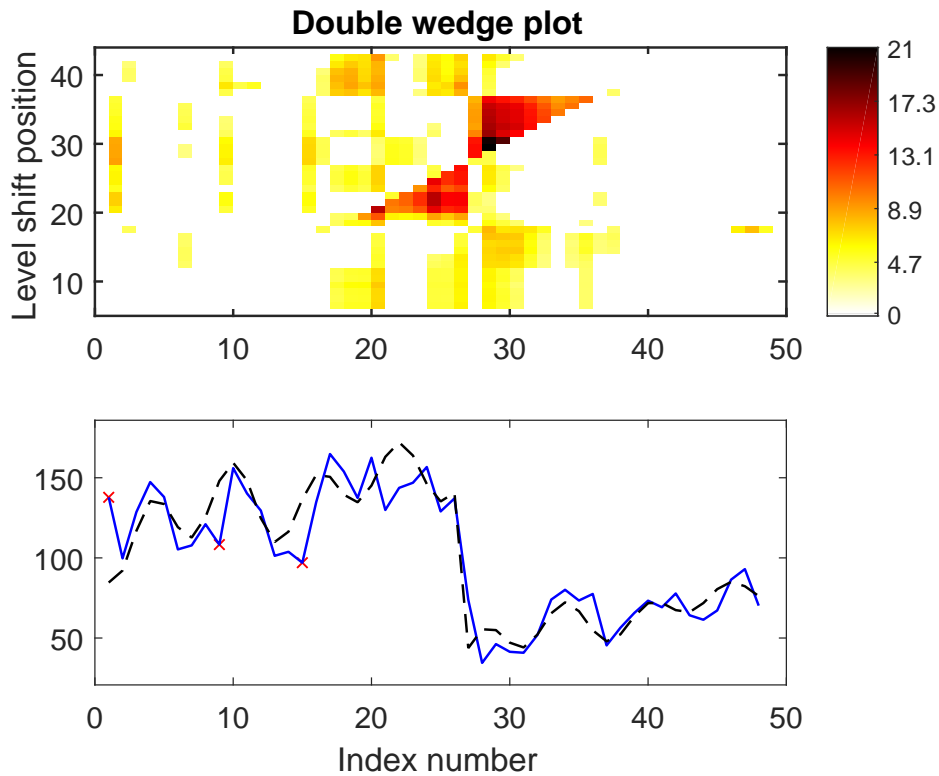


Figure 7: P12119085_KE_GB: double wedge plot (top) and observed and fitted values (bottom).

The robust fit to series P12119085-KE-GB (bottom panel of Figure 7) suggests three moderate outliers in positions 1, 9 and 15. The fit closely matches the level shift which

is therefore well captured. The double wedge plot in the top panel of Figure 7 has two wedges which point to a level shift position around 27-28. The local refinement step selects position $t = 27$.

Columns 2–4 of Table 1 show the coefficients of the final fit together with their t -statistics and p -values. Most coefficients are significant, and in particular the t -statistic of the height of the level shift is quite large with $|t| = 14.7$. This drop looks anomalous because in the period considered, Kenya was the only country of the East African Community (EAC) paying high European import duties on flowers and related products including CN 12119085. On the other hand, Kenya is the third largest exporter of cut flowers in the world. One would therefore check for a simultaneous upward level shift in an EAC country not paying import duties, which could point to a misdeclaration of origin.

Table 1: Coefficient estimates, t -statistics and p -values for series P12119085_KE_GB (columns 2-4) and P17049075_UA_LT (columns 5-7).

	P12119085_KE_GB			P17049075_UA_LT		
	Coeff	t -stat	p -values	Coeff	t -stat	p -values
$\hat{\alpha}_0$	115.27	25.6	0	55.14	14.3	0
$\hat{\alpha}_1$	1.59	5.80	0	0.90	4.52	0
$\hat{\beta}_{11}$	-2.83	-0.72	0.47	15.55	3.75	0.00056
$\hat{\beta}_{12}$	-12.42	-2.65	0.012	3.61	0.85	0.40
$\hat{\beta}_{21}$	-9.07	-1.95	0.059	-32.50	-7.64	0
$\hat{\beta}_{22}$	-22.60	-4.80	0	-16.06	-3.72	0.00061
$\hat{\gamma}_1$	-0.016	-3.72	0.00061	-0.023	-12.1	0
$\hat{\delta}_1$	-112.62	-14.7	0	-79.41	-13.9	0

Figure 8 shows the results for the second series, P17049075_UA_LT. The double wedge plot indicates the presence of a level shift around position 35. The local refinement yields the position $t = 34$. Interestingly, there is a reddish line right before the level shift. This is due to an outlier in position 32 which gets a red cross in the bottom panel of the figure. The double wedge plot also reveals a yellow strip at positions 29 and 30, indicating two less extreme outliers. Finally, the plot also shows some small reddish areas that correspond to

local irregularities, for instance observations 4, 5, 17 and 18 which are flagged as outliers in the bottom panel. Columns 5–7 of Table 1 list the coefficients of the final fit. Also here most coefficients are strongly significant.

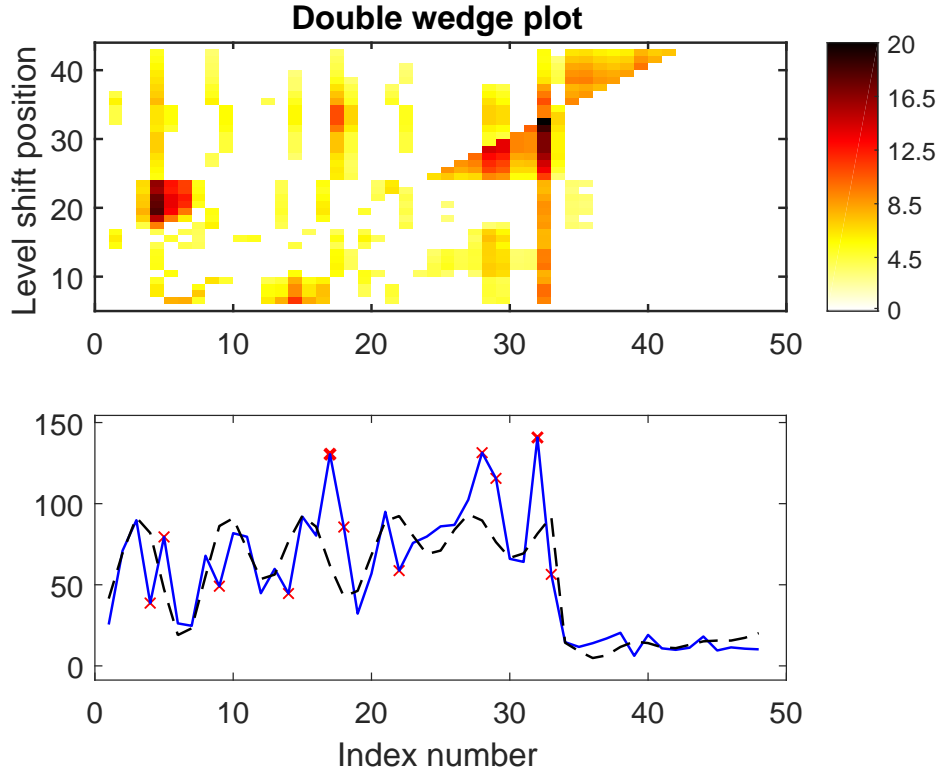


Figure 8: P17049075_UA_LT: double wedge plot (top) and observed and fitted values (bottom).

In this case the level shift might point to a different type of violation. The market of sugar and high-sugar-content products, such as CN code 17049075, is very restricted and regulated. The EU applies country-specific quotas for these products, with lower import duty for imports below the quota and a higher duty beyond this limit (tariff rate quotas). Therefore, it would be in an exporter’s interest to circumvent the quota by mislabeling this product as a somewhat related product that is not under surveillance. In this situation one would check for upward level shifts in related products from the same country.

Note that the t -values and p -values provided by LTS can help select a model. Table 1 fits model (2) with $A = 1$ (linear trend), $B = 2$ (two harmonics), and $G = 1$ (the amplitude varies linearly). If we increase A we find that a quadratic trend is insignificant, and the

same for increasing G . The t -values indicate that there is enough evidence for a 6-month seasonal effect but are less clear on the question whether B should be increased further for these short time series. In any case the detection of the level shift turns out to be stable as a function of B here.

5 Comparison with other methods

We now compare our results with those obtained by the nonparametric method introduced by Fried (2004) and Fried and Gather (2007) for robust filtering of time series. For this we used the function `robust.filter` from the R package `robfilter` of Fried et al. (2012). The robust fitting methods are applied to a moving time window of size `width`, which needs to be an odd number.

Table 2: P_12119085_KE_GB: Positions of level shifts and outliers detected by a nonparametric time series filter, using different window widths.

Window width	Level shift position(s)	Outlier position(s)
3	-	[10, 16, 17, 37, 38, 46, 47]
5	-	[16, 17, 18, 47]
7	[27]	[17, 18]
9	[27, 37]	-
11	[27]	-

Tables 2 and 3 report the position of the level shift(s) and outlier(s) detected with all default options and various choices of window widths. We also tested different robust choices for the trend and scale estimation and some values for the `adapt` option which adapts the moving window width, with similar results.

Figures 9(a) and (b) show the resulting fits obtained by the nonparametric filter, for widths giving rise to the detection of a level shift (width = 7 for P_12119085_KE_GB and width = 11 for P_17049075_UA_LT). In the first series we see that the level shift is detected well for the appropriate width, but the fit itself is not as tight. Also in the second series

Table 3: P_17049075_UA_LT: Positions of level shifts and outliers detected by a nonparametric time series filter, using different window widths.

Window width	Level shift position(s)	Outlier position(s)
3	-	[2, 15, 44]
5	-	[15, 16, 17, 28, 30, 31, 33, 39, 40, 41]
7	-	[30, 31, 33, 34]
9	-	[30, 31, 33, 34, 35]
11	[30]	[32]

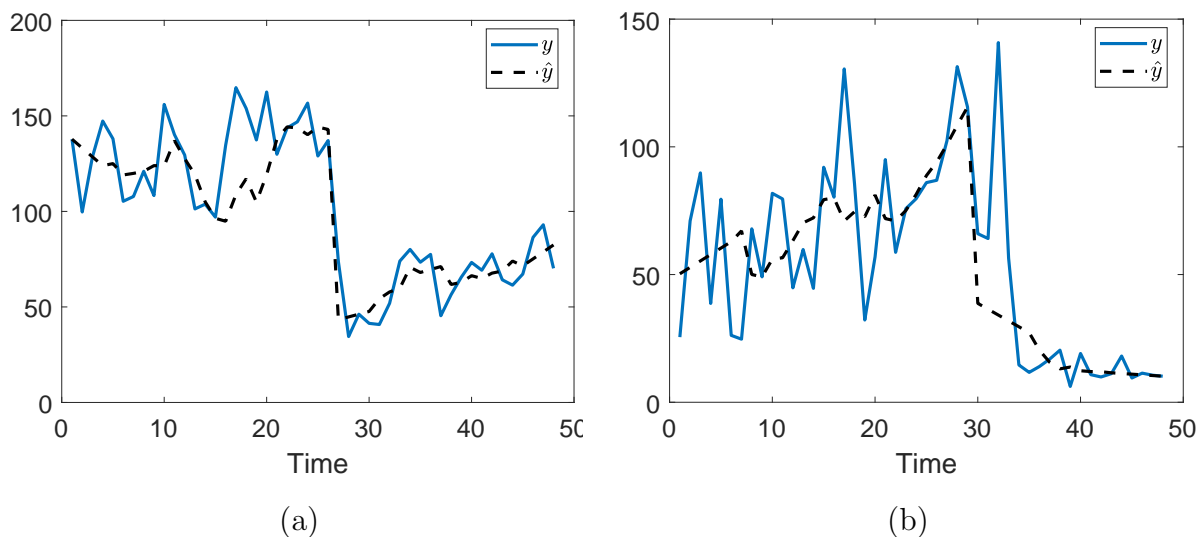


Figure 9: Fits obtained by a nonparametric time series filter for (a) P12119085_KE_GB; (b) P17049075_UA_LT.

a reasonable level shift position is found but the fit is not that close to the series. This can be explained by the fact that a nonparametric method has no prior knowledge about the data as it has to work on any data set, whereas our parametric model benefits from knowledge about the typical behavior of trade time series. In that sense the comparison is not entirely fair.

We also run the well-known X-13 ARIMA-SEATS method (Findley et al., 1998; U.S. Census Bureau, 2017) on both trade time series, by means of the R package `seasonal` (Sax, 2017) which

interfaces X-13. This method fits an ARIMA model with a seasonal component. In addition to the coefficients required for the ARIMA model, X-13 has T additional parameters for level shifts, one at each time point $t = 1, \dots, T$, plus T parameters for additive outliers (AO). Their coefficients are estimated by stepwise regression, so most of them remain zero. For detecting isolated outliers, i.e. outliers surrounded by non-outlying values, this approach works quite well.

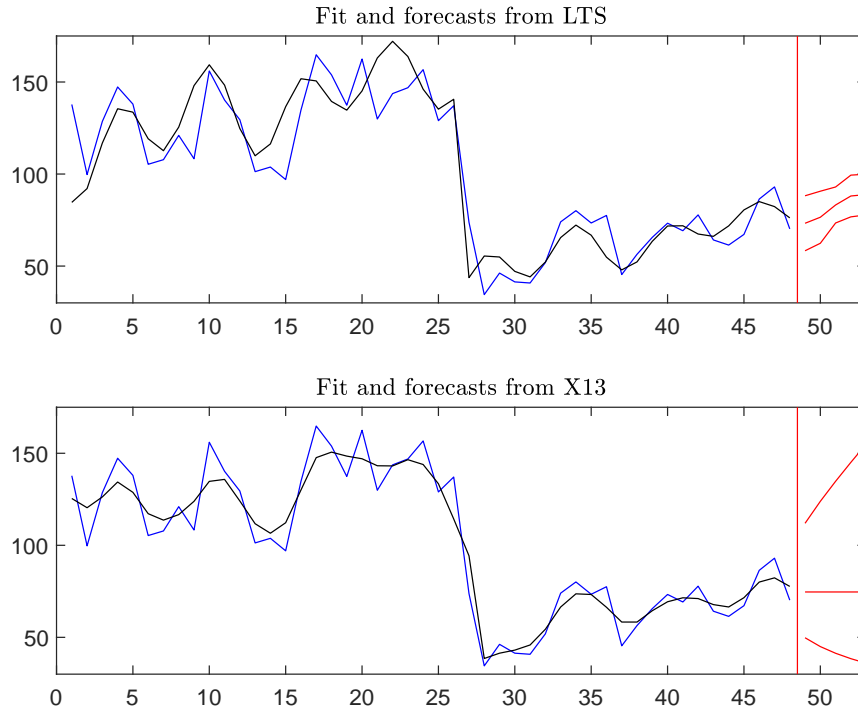


Figure 10: Trade series P12119085_KE_GB: time series (blue), fit (black) and forecast (red) obtained by LTS (top panel) and X-13 (bottom panel).

Figure 10 shows the X-13 fit to the trade series P12119085_KE_GB in the lower panel, with the LTS fit in the upper panel for comparison. Figure 11 does the same for P17049075_UA_LT. The blue curves are the time series, and the fits are in black. In both cases X-13 does detect the level shift. It obtains the model (0 1 1) which only has a moving average and no seasonal component. As a result its forecast (shown in red) has no seasonal component either. Note that in Figure 10 the 90% tolerance band around the forecast is much wider for X-13 than for LTS.

Let us now return to the airline data with contamination 1 described in Section 3. The

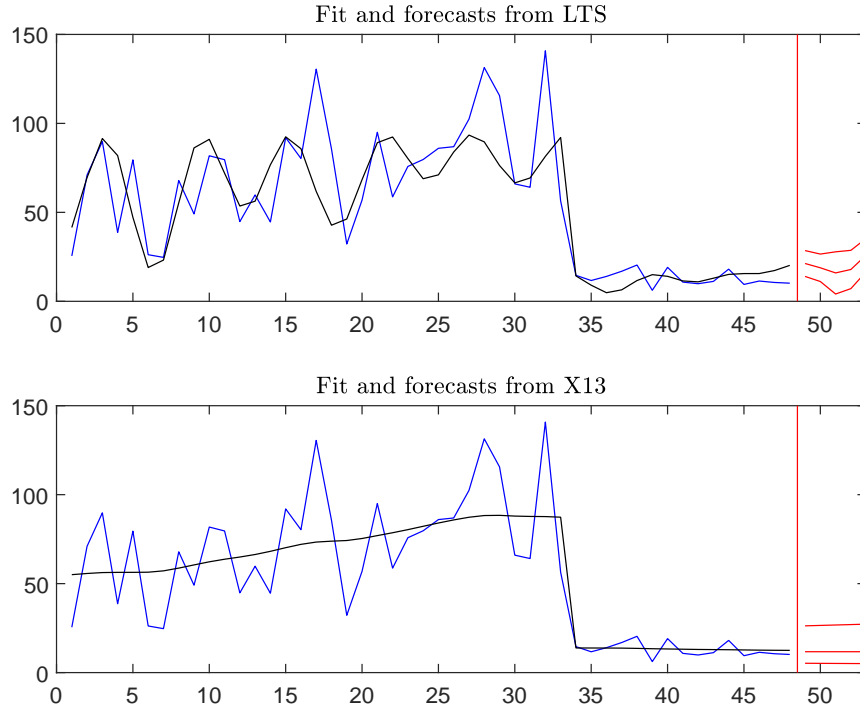


Figure 11: Trade series P17049075_UA_LT: time series (blue), fit (black) and forecast (red) obtained by LTS (top panel) and X-13 (bottom panel).

results of LTS were shown in Figure 3. We now apply X-13 to it. The R-code and output are available in Section A.1 of the Supplementary Material. The model found by X-13 is ARIMA with $(1\ 1\ 0)(0\ 1\ 0)$ whereas for the uncontaminated airline data it was $(0\ 1\ 1)(0\ 1\ 1)$. In this example the X-13 fit has 7 nonzero coefficients describing level shifts, and 1 nonzero coefficient for an AO outlier. The bottom panel of Figure 12 shows the time series and the X-13 fit which accommodates the outliers. On the other hand, the LTS fit in the top panel follows the pattern of the majority of the data, so the outliers have large residuals from it. Also the forecasts are quite different: those of LTS increase and have a narrow tolerance band, while those of X-13 slightly decrease and have wide tolerance bands. For the uncontaminated airline data (that is, without outliers) the forecasts and tolerance bands of LTS and X-13 were very similar.

Note that X-13 fits each set of consecutive outliers by a level shift at the start and a level shift afterward. That description is indeed equivalent to the consecutive outliers representation. Our point is that accommodating the outliers gives a close fit to the observed

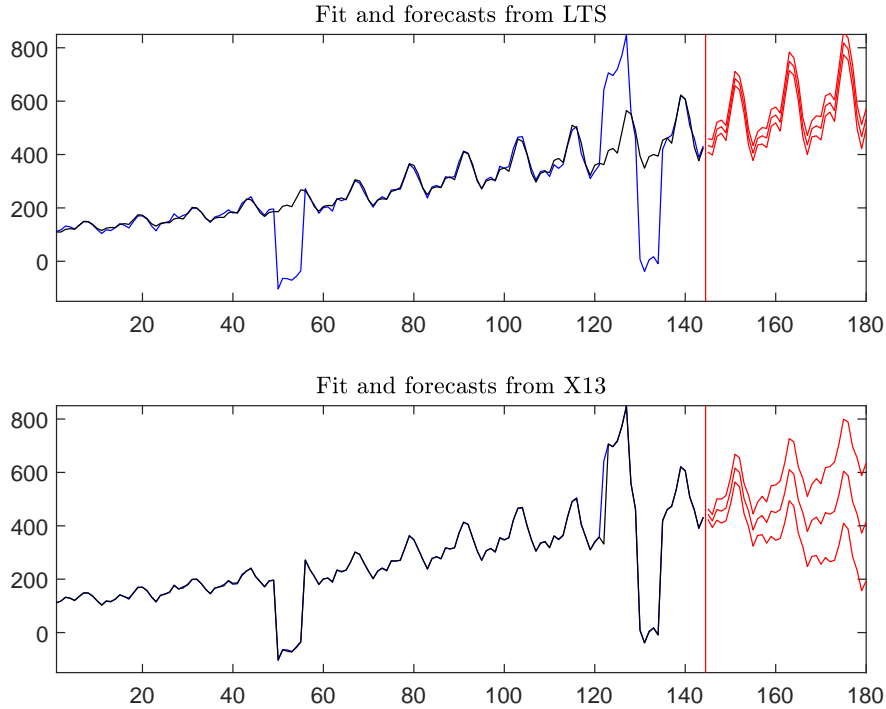


Figure 12: Airline data with contamination 1: time series (blue), fit (black) and forecast (red) obtained by LTS (top panel) and X-13 (bottom panel).

time series, but as we see here it can inflate the forecast band.

On the airline data without outliers, X-13 automatically log transforms the data before fitting it. On the airline data with contamination it does not, because the time series contains at least one negative value. (Other transformations would be possible, but in automatic mode X-13 only considers the log transform.) In this example the negative values were due to outliers, but in fact many trade time series in the EU database have at least one zero value, correctly reflecting that a certain product was not imported for a month, which will also prevent X-13 from transforming the data.

To investigate this issue further, we looked at two ways to make the contaminated airline data positive. The first was to add a constant so that the minimum of the contaminated time series becomes 1 (we also tried 5, 10 and 50). The second was to truncate the series from below at 1 (or 5, 10, 50) so the downward outliers of contamination 1 remain visible. However, in none of these cases did X-13 carry out a logarithmic transform, indicating that its transformation criterion was affected by the outliers.

Also note that the outliers have a large magnitude in this example. In response to a referee request we also provide an example with a level shift that is smaller than the seasonal component, in Section A.2 of the Supplementary Material.

6 The case of several level shifts

Our basic model (2) only covers the situation where at most one level shift occurs, which is a reasonable assumption for short time series. When several level shifts can occur, we first apply our approach to the original time series. If it detects a level shift we can modify the time series by undoing the break, that is, subtract $\hat{\delta}_1$ from all y_t to the right of the level shift, after which one can search for the next level shift, and so on. A detailed example of this procedure is shown in subsection A.3 of the Supplementary Material.

7 Conclusions and outlook

We have introduced a new robust approach to model and monitor nonlinear time series with possible level shifts. A fast algorithm was developed and applied to several real and artificial datasets. We also proposed a new graphical display, the double wedge plot, which visualizes the possible presence of a level shift as well as outliers. This graph requires no additional computation as it is an automatic by-product of the estimation. Our approach thus allows to automatically flag outlying measurements and to detect a level shift, which is important in fraud detection as these may be indications of unauthorized transactions. At the European Joint Research Centre, this methodology was validated by comparing its results to those of visual inspection of many trade series by subject-matter experts.

Supplementary Material

The supplementary material to this paper contains some R code and worked-out examples.

Appendix

Here we prove that a C-step (as used in the first step of the NLTS algorithm) can only decrease the LTS objective function.

Let $H^{(k)}$ be the current h -subset with its corresponding nonlinear LS coefficients $\hat{\theta}^{(k)} = (\{\hat{\alpha}^{(k)}\}, \{\hat{\beta}^{(k)}\}, \{\hat{\gamma}^{(k)}\}, \hat{\delta}_1^{(k)}, \hat{\delta}_2)$ and objective function $L^{(k)} = \sum_{t \in H^{(k)}} r_{(t)}^2(\hat{\theta}^{(k)})$.

Now consider $H^{(k+1)}$, the h -subset which contains the h observations with smallest squared residual with respect to $\hat{\theta}^{(k)}$. Then by construction

$$\sum_{t \in H^{(k+1)}} r_{(t)}^2(\hat{\theta}^{(k)}) \leq \sum_{t \in H^{(k)}} r_{(t)}^2(\hat{\theta}^{(k)}) = L^{(k)}. \quad (9)$$

The ALS step A then yields $\hat{\theta}^{(k+0.5)} = (\{\hat{\alpha}^{(k+1)}\}, \{\hat{\beta}^{(k)}\}, \{\hat{\gamma}^{(k+1)}\}, \hat{\delta}_1^{(k+1)}, \hat{\delta}_2)$. Since it is the LS solution of the linear model (5),

$$\sum_{t \in H^{(k+1)}} r_{(t)}^2(\hat{\theta}^{(k+0.5)}) \leq \sum_{t \in H^{(k+1)}} r_{(t)}^2(\hat{\theta}^{(k)}). \quad (10)$$

Next, ALS step B yields $\hat{\theta}^{(k+1)} = (\{\hat{\alpha}^{(k+1)}\}, \{\hat{\beta}^{(k+1)}\}, \{\hat{\gamma}^{(k+1)}\}, \hat{\delta}_1^{(k+1)}, \hat{\delta}_2)$ with

$$L^{(k+1)} = \sum_{t \in H^{(k+1)}} r_{(t)}^2(\hat{\theta}^{(k+1)}) \leq \sum_{t \in H^{(k+1)}} r_{(t)}^2(\hat{\theta}^{(k+0.5)}). \quad (11)$$

Combining (9)-(11) yields

$$L^{(k+1)} \leq L^{(k)}$$

so the new h -subset $H^{(k+1)}$ has an objective function that is less than or equal to that of $H^{(k)}$. Note that the only way to obtain equality is if no coefficients have changed, in which case the iteration stops.

References

References

Agostinelli, C., Leung, A., Yohai, V., Zamar, R., 2015. Robust estimation of multivariate location and scatter in the presence of cellwise and casewise contamination. *Test* 24, 441–461.

- Barabesi, L., Cerasa, A., Perrotta, D., Cerioli, A., 2016. Modelling international trade data with the Tweedie distribution for anti-fraud and policy support. *European Journal of Operational Research* 258, 1031–1043.
- Bianco, A. M., Garca Ben, M., Martnez, E. J., Yohai, V. J., 2001. Outlier detection in regression models with ARIMA errors using robust estimates. *Journal of Forecasting* 20 (8), 565–579.
- Box, G. E. P., Jenkins, G. M., 1976. *Time Series Analysis: Forecasting and Control*. Holden Day, San Francisco.
- Čížek, P., 2005. Least trimmed squares in nonlinear regression under dependence. *Journal of Statistical Planning and Inference* 136, 3967–3988.
- Čížek, P., 2008. General trimmed estimation: robust approach to nonlinear and limited dependent variable models. *Econometric Theory* 24 (6), 1500–1529.
- Croux, C., Rousseeuw, P. J., 1992. A class of high-breakdown scale estimators based on subranges. *Communications in Statistics - Theory and Methods* 21, 1935–1951.
- Findley, D. F., Monsell, B. C., Bell, W. R., Otto, M. C., Chen, B. C., 1998. New capabilities of the X-12-ARIMA seasonal adjustment program. *Journal of Business and Economic Statistics* 16, 127–177.
- Fried, R., 2004. Robust filtering of time series with trends. *Journal of Nonparametric Statistics* 16 (3-4), 313–328.
- Fried, R., Gather, U., 2007. On rank tests for shift detection in time series. *Computational Statistics & Data Analysis* 52 (1), 221–233.
- Fried, R., Schettlinger, K., Borowski, M., 2012. Package ‘robfilter’. CRAN, URL <https://CRAN.R-project.org/package=robfilter>.
- Galeano, P., Peña, D., 2013. Finding outliers and unexpected events in linear and nonlinear possible multivariate time series data. In: Becker, C., Fried, R., Kuhnt, S. (Eds.), *Robustness and Complex Data Structures. Festschrift in Honour of Ursula Gather*. Springer, pp. 255–273.

- Gervini, D., Yohai, V. J., 2002. A class of robust and fully efficient regression estimators. *Annals of Statistics* 30, 583–616.
- Pison, G., Van Aelst, S., Willems, G., 2002. Small sample corrections for LTS and MCD. *Metrika* 55, 111–123.
- Rousseeuw, P., 1984. Least median of squares regression. *Journal of the American Statistical Association* 79, 871–880.
- Rousseeuw, P., Hubert, M., 2018. Anomaly detection by robust statistics. *WIREs Data Mining and Knowledge Discovery* e1236.
- Rousseeuw, P., Leroy, A., 1987. *Robust Regression and Outlier Detection*. Wiley-Interscience, New York.
- Rousseeuw, P., Van Driessen, K., 2006. Computing LTS regression for large data sets. *Data Mining and Knowledge Discovery* 12, 29–45.
- Salini, S., Cerioli, A., Laurini, F., Riani, M., 2015. Reliable robust regression diagnostics. *International Statistical Review* 84, 99–127.
- Sax, C., 2017. Package ‘seasonal’: R Interface to X-13-ARIMA-SEATS. CRAN, URL <https://CRAN.R-project.org/package=seasonal>.
- Stromberg, A., 1993. Computation of high breakdown nonlinear regression parameters. *Journal of the American Statistical Association* 88, 237–244.
- Stromberg, A., Ruppert, D., 1992. Breakdown in nonlinear regression. *Journal of the American Statistical Association* 87, 991–997.
- U.S. Census Bureau, 2017. X-13ARIMA-SEATS Reference Manual, Version 1.1. URL <http://www.census.gov/srd/www/x13as>.

SUPPLEMENTARY MATERIAL

A.1 R-code for the airline data with contamination 1

```
> library("seasonal")
> library("forecast")
> y = AirPassengers
> y[50:55] = y[50:55]-300
> y[122:127] = y[122:127]+300
> y[130:134] = y[130:134]-400
> out = seas(y, forecast.save = "forecasts")
> summary(out)
```

Coefficients:

	Estimate	Std. Error	z value	Pr(> z)	
LS1953.Feb	-294.29555	6.88904	-42.719	< 2e-16	***
LS1953.Aug	304.98444	6.88904	44.271	< 2e-16	***
A01959.Feb	310.47628	7.17862	43.250	< 2e-16	***
LS1959.Mar	329.79392	11.04369	29.863	< 2e-16	***
LS1959.Aug	-285.79555	6.88904	-41.486	< 2e-16	***
LS1959.Oct	-404.90220	6.88904	-58.775	< 2e-16	***
LS1960.Mar	385.12429	14.05921	27.393	< 2e-16	***
LS1960.Apr	47.91993	10.15210	4.720	2.36e-06	***
AR-Nonseasonal-01	-0.30043	0.08324	-3.609	0.000307	***

SEATS adj. ARIMA: (1 1 0)(0 1 0) Obs.: 144 Transform: none

```
> forec = series(out, c("forecast.forecasts", "s12"))
> forec[1:144,1] = y
> plot(forec[,1],ylim=c(-100,800),col="blue")
> fit = trend(out) + forecast::seasonal(out)
```

```

> lines(fit,col="black")
> lines(forec[,2],col="red") # forecast
> lines(forec[,3],col="red")
> lines(forec[,4],col="red")

```

A.2 Effect of a small level shift

For this example the time series has length $T = 150$ and it is generated according to model (2) with $A = 1$, $B = 3$, $G = 1$. In particular $\alpha_0 = 1$, $\alpha_1 = 1$, $\beta_{1,1}, \beta_{1,2}, \beta_{2,1}, \beta_{2,2}, \beta_{3,1}, \beta_{3,2}] = [20, -20, 12, -12, 4, -4]$ and $\gamma_1 = 8.88$. There is one level shift of height $\delta_1 = 13,000$ at time $\delta_2 = 40$. The error term is generated with a signal to noise ratio of 20.

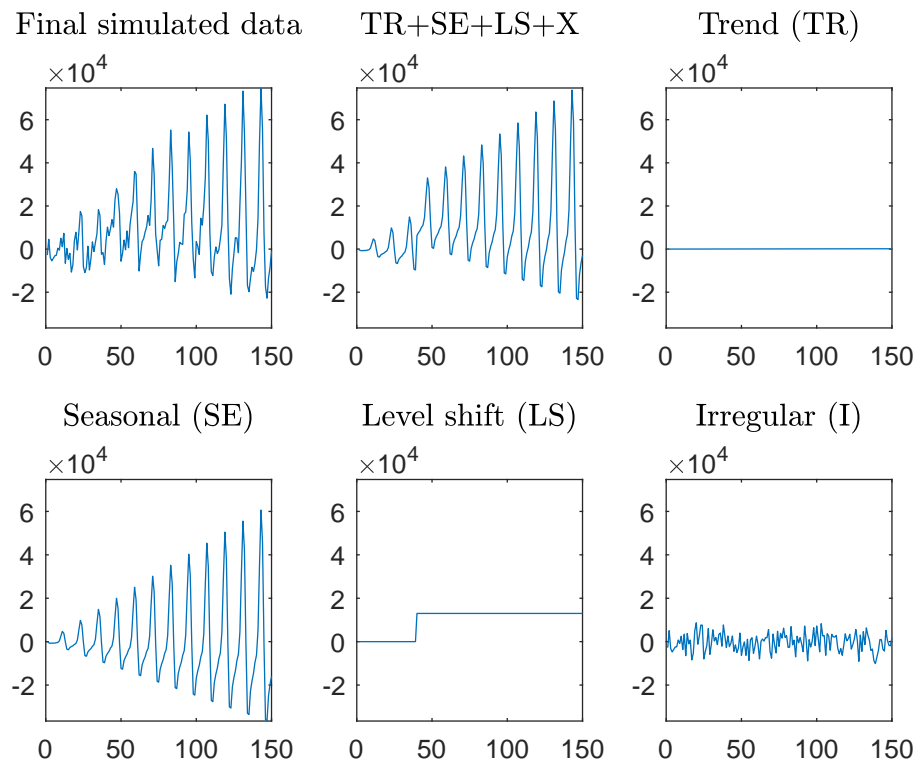


Figure 13: Components of the generated data set of Section A.2.

All the components in Figure 13 are shown using the same vertical scale so their relative size can be seen. The trend is increasing but appears horizontal if we compare it to the magnitude of the other components. We see that the level shift is smaller than the seasonal

component, and similar in size to the spread of the error term (called “irregular” in the plot). The time series will be made available on [/www.riani.it/rprh/](http://www.riani.it/rprh/).

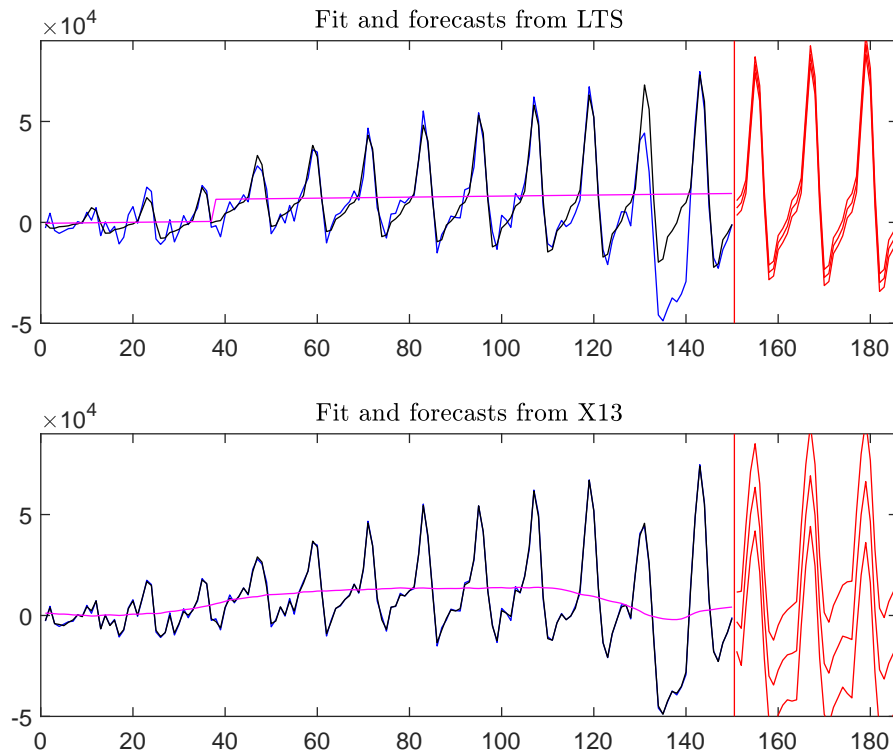


Figure 14: Data of Section A.2: time series (blue), trend (purple), overall fit (black), and forecast (red) obtained by LTS (top) and X-13 (bottom).

After generating this time series we also create a stretch of outliers by subtracting 29,000 from the values at times in $[131, 140]$. The top panel of Figure 14 shows the result of the LTS procedure, with the time series (blue), the estimated trend including the estimated level shift (purple), the overall fit (black) and the forecast (red). The level shift is clearly visible, and the outliers stand out by their sizeable residual (look at $y_t - \hat{y}_t$ in this plot) for t in $[131, 140]$.

The bottom panel shows the X-13 fit, which does not detect the level shift. Instead there is a mild increase in the X-13 trend where the level shift takes place, followed by a mild decrease in the vicinity of the stretch of outliers. The X-13 forecast is stationary, whereas the LTS forecast has increasing seasonal fluctuations in line with the underlying model. The tolerance band around the forecast is much wider for X-13 than for LTS.

A.3 More than one level shift

We now consider an example with two level shifts. Starting from the original airline data, we subtract 100 from the values at times in $[1, 30]$ and add 200 at the times in $[100, 144]$ which creates level shifts at times 31 and 100.

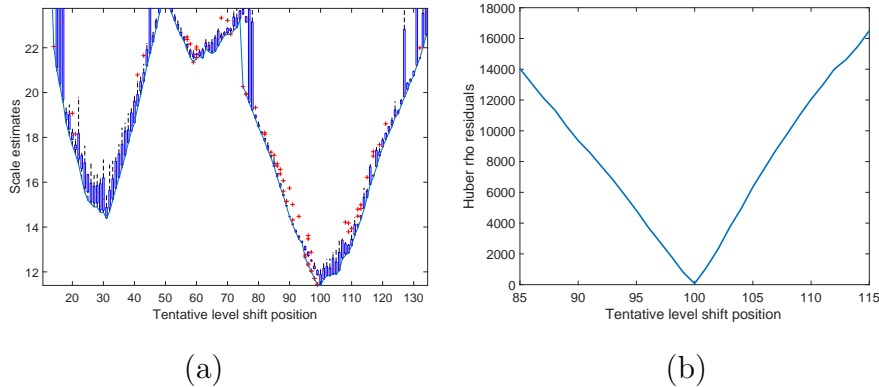


Figure 15: First estimation of a level shift in the data of A.3: (a) boxplots of the 20 lowest objective function values attained at each $t_{(s)}$; (b) local improvement of the shift position estimate.

Applying LTS to these contaminated data correctly detects the level shift at time 100, as seen in Figure 15 with the objective function and its local refinement (similar to Figure 5). The resulting double wedge plot in the top panel of Figure 16 actually reveals both level shifts. Interestingly, the LTS fit in the lower panel of Figure 16 flags the first 30 points as a stretch of outliers.

In the next step we undo the level shift that was found, by subtracting $\hat{\delta}_1 = 194.47$ from y_t in all $t \geq \hat{\delta}_2 = 100$. To this modified time series we again apply LTS, which now correctly detects the level shift at time 31 as seen in Figure 17. The resulting double wedge plot in Figure 18 now shows only this level shift (since the other one has been removed). The final fit no longer shows any outliers. If we undo also the second level shift and run LTS again, no more level shifts are found.

We also ran examples where the level shifts had roughly the same size and with more than two level shifts, with similar results.

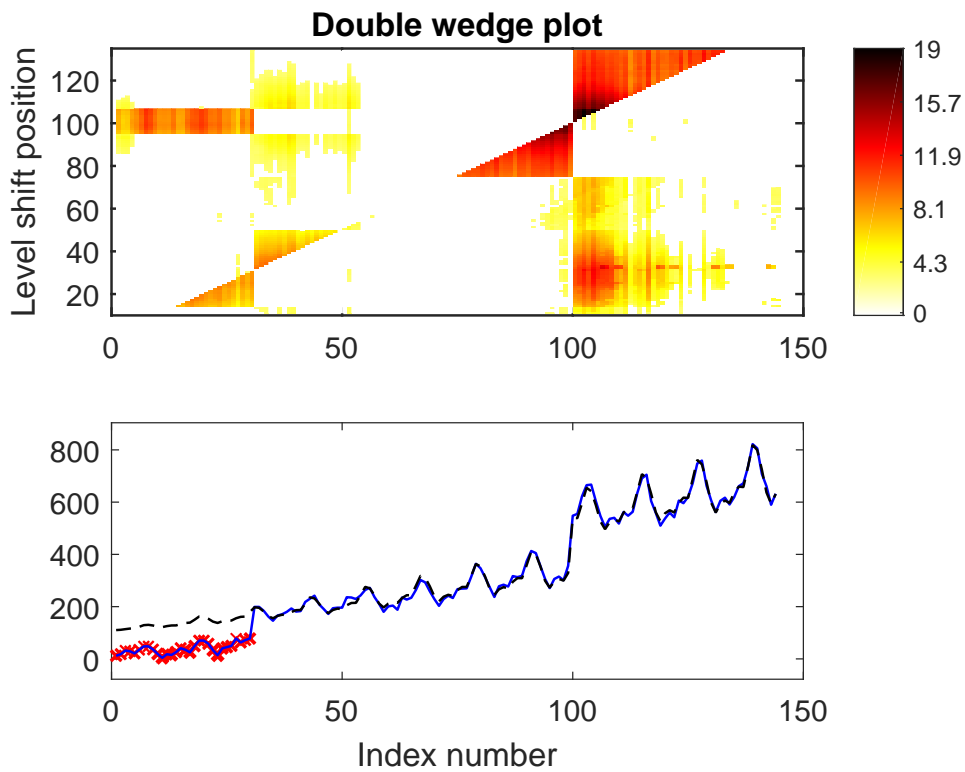


Figure 16: First fit to the data of Section A.3.

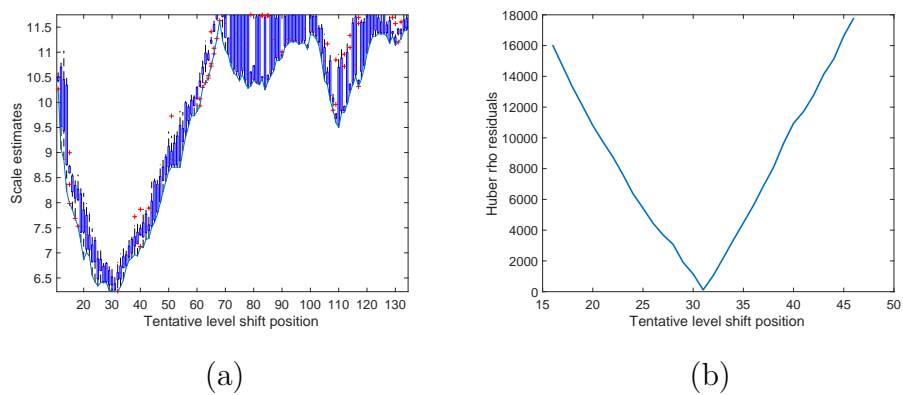


Figure 17: Estimation of a level shift in the data of A.3, after undoing the first level shift found.

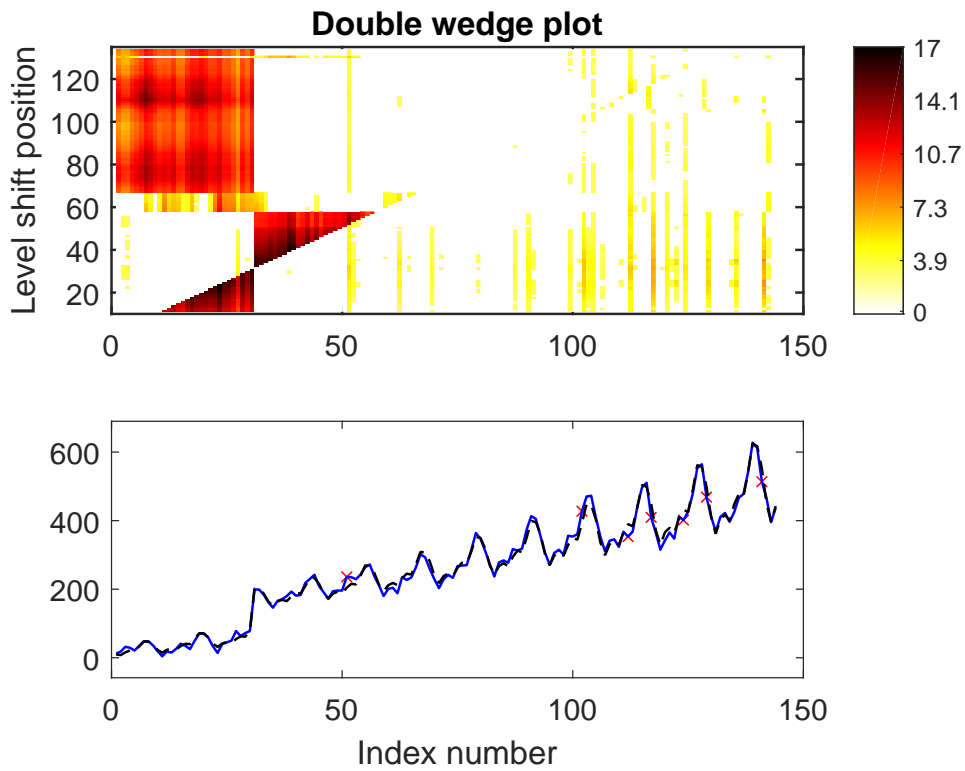


Figure 18: Fit to the data of A.3 after undoing the first estimated level shift.